RESEARCH ARTICLE

Terrestrial pyrogenic carbon export to fluvial ecosystems: Lessons learned from the White Nile watershed of East Africa

David T. Güereña[1], Johannes Lehmann[1,2], Todd Walter[3], Akio Enders[1], Henry Neufeldt[4], Holiance Odiwour[4], Henry Biwott[4], John Recha[5], Keith Shepherd[4], Edmundo Barrios[4], and Chris Wurster[6,7]

[1]Department of Crop and Soil Sciences, Cornell University, Ithaca, New York, USA, [2]Atkinson Center for a Sustainable Future, Cornell University, Ithaca, New York, USA, [3]Department of Biological and Environmental Engineering, Cornell University, Ithaca, New York, USA, [4]World Agroforestry Centre (ICRAF), Nairobi, Kenya, [5]The International Livestock Research Institute, Nairobi, Kenya, [6]College of Science, Technology and Engineering, James Cook University, Townsville, Queensland, Australia, [7]Centre for Tropical Environmental and Sustainability Sciences, James Cook University, Townsville, Queensland, Australia

Abstract Pyrogenic carbon (PyC) is important because of its role in the global organic C (OC) cycle and in modifying soil properties. However, our understanding of PyC movement from terrestrial to fluvial ecosystems is not robust. This study examined (i) whether erosion or subsurface transport was more important for PyC export from headwaters, (ii) whether PyC was exported preferentially to total OC (TOC), and (iii) whether the movement of PyC from terrestrial to aquatic ecosystems provides an explanation for the coupling of PyC and non-PyC observed in rivers at a global scale. In the Guineo-Congolian highland forest region of western Kenya, duplicate catchments with sizes of 1–12 ha were equipped with stream gauges in primary forest and adjacent mixed agricultural landscapes that were cleared by fire 10, 16, or 62 years before. Stream water samples were taken weekly throughout 1 year and compared with runoff to assess PyC movement. Additional stream samples were taken from all major tributaries of the White Nile watershed of Lake Victoria. PyC was not found to be preferentially eroded relative to TOC or non-PyC, as topsoil (0–0.15 m) PyC concentrations ($6.3 \pm 0.3\%$ of TOC; means and standard errors) were greater than runoff sediment ($1.9 \pm 0.4\%$) and dissolved PyC concentrations ($2.0 \pm 0.4\%$, $n = 252$). In addition, PyC proportions in eroded sediment were lower than and uncorrelated ($r^2 = 0.04$; $P = 0.14$) with topsoil PyC. An enrichment of PyC was found with depth in the soil, from $6.3 \pm 0.3\%$ of TOC in the topsoil (0–0.15 m) to $12.3 \pm 0.3\%$ of TOC at 1–2 m. Base flow PyC proportions of TOC correlated well with subsoil PyC ($r^2 = 0.57$; $P < 0.05$) but not with topsoil PyC ($r^2 = 0.18$; $P > 0.05$). Similar PyC proportions were found in the studied headwater streams ($2.7 \pm 0.2\%$), their downstream inflow into Lake Victoria (3.7%), the other nine major rivers into Lake Victoria ($4.9 \pm 0.8\%$), and its outflow into the White Nile (1.1%). A strong positive correlation between dissolved PyC and non-PyC ($r^2 = 0.91$; $P < 0.0001$) in the headwater streams reflect relationships previously seen for a range of globally important rivers, and contrasts with a negative relationship for suspended sediments ($r^2 = -0.5$; $P < 0.0001$). The estimated PyC export from the Lake Victoria watershed of $11\,\mathrm{Gg\,yr^{-1}}$ may therefore originate to a large extent from subsoil pathways in dissolved form that appeared to be an important source of PyC in aquatic environments and may explain the coupling of PyC and non-PyC at a global scale.

1. Introduction

Vegetation fires can deposit substantial quantities of pyrogenic carbon (PyC) in terrestrial environments [*Crutzen and Andreae*, 1990; *Kuhlbusch et al.*, 1996]. The global PyC production is estimated to lie between 8 and $270\,\mathrm{Tg\,C\,yr^{-1}}$, of which 40% is generated from open biomass burning [*Bird et al.*, 2015; *Forbes et al.*, 2006; *Kuhlbusch and Crutzen*, 1995; *Ramanathan and Carmichael*, 2008]. High soil PyC contents have been found in fire-dominated ecosystems with up to 35% of soil organic carbon (SOC) in the U.S. [*Jauss et al.*, 2014; *Skjemstad et al.*, 2002], 45% in German chernozemic soils [*Schmidt et al.*, 1999], and 82% in Australia [*Lehmann et al.*, 2008]. Some authors have therefore hypothesized that PyC deposits serve as a terrestrial C sink [*Goldberg*, 1985]. However, the biogeochemical fate of these PyC deposits within and losses from terrestrial ecosystems are still poorly quantified [*Czimczik and Masiello*, 2007]. Physical export of PyC from the soil and its input into aquatic ecosystems is an important and little investigated fate of PyC [*Jaffé et al.*, 2013; *Schmidt and Noack*, 2000] despite high global estimates of fluvial dissolved and particulate PyC movement into oceans of 44–$108\,\mathrm{Tg\,C\,yr^{-1}}$ [*Bird et al.*, 2015].

Transport of PyC by erosion may be significant [*Major et al.*, 2010] and PyC has been found to preferentially erode with surface water in comparison to non-PyC [*Rumpel et al.*, 2006a]. For major South American river systems, fluvial export was found to be more important for PyC than non-PyC and attributed to preferential export of PyC during high water discharge [*Dittmar et al.*, 2012]. At the same time, PyC in the main global rivers appears to be closely coupled to non-PyC [*Jaffé et al.*, 2013] which is not easily explained by preferential PyC export through water erosion. However, different flow paths from terrestrial to fluvial systems have not been compared on a watershed scale and may provide explanations for observations at the global scale.

In addition to erosion, leaching of surface-deposited PyC contributes to a loss of surface PyC and to an export of PyC to fluvial ecosystems. *Major et al.* [2010] found dissolved and particulate PyC in leachate collected at a depth of 0.3 m from an Oxisol in Columbia during the first leaching events after PyC deposition to soil. Similarly, *Riedel et al.* [2014] found evidence of OC forms originating from applied PyC leaching out of soil columns. Some studies have documented a relative enrichment of PyC as a proportion of SOC in the subsoil [*Dai et al.*, 2005; *Jauss et al.*, 2014; *Knicker et al.*, 2012], while others do not show any subsurface enrichment [*Alexis et al.*, 2012]. On former peat lands *Leifeld et al.* [2007] found up to 69% of the total PyC content below the plough layer. This suggests that leaching might constitute an important mechanism for PyC losses from surface soils. However, we are not aware of published studies that evaluate PyC redistribution through movement into the subsoil at the scale of headwater catchments and investigate a possible connection to stream water.

It is also not known under what conditions the documented erosion or leaching of PyC represent losses from terrestrial ecosystems into stream water or when they lead to translocations within the landscape. Redistribution within the watershed could explain differences seen between plot and global scale studies. Within a catchment, mineral soil sediments dislodged and transported by water are often redeposited before they reach the bottom of a slope or exit the watershed [*Polyakov and Lal*, 2004]. Particle density differences between PyC and mineral soil might change this dynamic, because the particle density of PyC is lower than the particle density of the mineral matter within soil [*Brewer et al.*, 2009]. Less dense particles may be more vulnerable to erosion, which should result in preferential erosion of freshly deposited PyC relative to mineral soil. However, PyC can sorb to mineral surfaces [*Joseph et al.*, 2010], which was shown to reduce the susceptibility of PyC to erosion [*Rumpel et al.*, 2006b]. Such PyC-mineral associations may form in soil over time as illustrated by the virtual lack of net decreases in soil PyC stocks between 30 and 100 years after deposition which was associated with increases of iron, silicon, and aluminum on PyC particles [*Nguyen et al.*, 2008]. It is not clear whether these changes in PyC-mineral associations over decadal time scales alter the PyC susceptibility to erosion or leaching and thereby also alter PyC export to fluvial systems or its redistribution within headwaters [*Hockaday et al.*, 2006].

Therefore, this study investigated the movement of PyC within terrestrial ecosystems as well as from terrestrial to fluvial ecosystems in headwaters of the Guineo-Congolian highland forest in western Kenya and the Lake Victoria watershed. It aimed at providing insights into the origin of aquatic PyC and the reason for its coupling with non-PyC at the global scale. The objectives of this project were (1) to quantify the magnitude and pathways of terrestrial PyC movement at the scale of headwaters as a function of time from an initial fire event and (2) to compare mobilization and fluxes of PyC and non-PyC from headwaters to larger rivers. The specific hypotheses of the project were the following: (a) Erosion is the dominant pathway of PyC translocation within and export from terrestrial ecosystems and (b) PyC is preferentially eroded relative to non-PyC.

2. Methods

2.1. Field Site

The studied catchments in the Kapchorwa region of western Kenya form part of the headwaters of the Yala River that flows into the northeastern portion of Lake Victoria near the Kavirondo Gulf. The field site is located in the Nandi district approximately 60 km northeast of Lake Victoria at longitude 35°0'00"E and latitude 0°10'0"N. The mean elevation is 1800 m with a mean annual precipitation of 2000 mm and a mean annual temperature of 23°C. Rainfall is bimodal with approximately 1200 mm of rainfall falling between April and June and approximately 800 mm between August and October. Soils at the site are classified as humic Nitisol [*Sombroek et al.*, 1982] weathering from granite and gneiss [*Schluter and Hampton*, 1997] and have a texture of 45–49% clay, 15–25% silt, and 26–40% sand [*Kimetu et al.*, 2008]. The original vegetation in the region consists of highland rainforest and the remaining forest is the easternmost extension of the Guineo-Congolian forest belt [*Wass*, 1995].
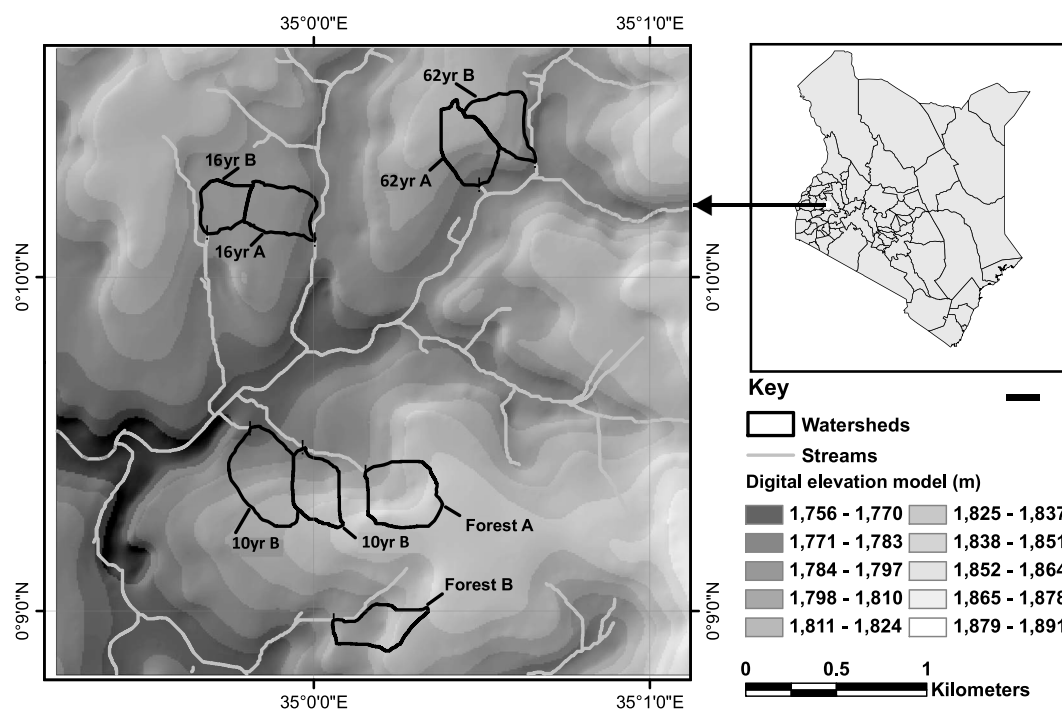
Figure 1. Elevation and slope maps of the study area in the Kapchorwa region of western Kenya and the approximate location within Kenya (adapted from *Recha et al.* [2013]).

The Kapchorwa catchments are first-order streams and follow a gradient of land use change. Two adjacent catchments (A and B) each were identified in the forest (called catchments FA and FB) as well as on lands cleared, burned, and converted to agriculture in the years 2002 (called young agricultural catchments, 10A and 10B), 1996 (called medium agricultural catchments, 16A and 16B), and 1950 (called old agricultural catchments, 62A and 62B) with sizes between 1 and 12 ha (Figure 1; Table S1 in the supporting information). The two catchments per land use (A and B) served as replicate observations but results were shown for each individually throughout the study. These time series or so-called chronosequences substitute time for space and have to be carefully selected to assure similar soils, hydrology, and vegetation before the change and similar land use history including vegetation burning thereafter [*Huggett*, 1998]. The selection of the catchments was made after multiyear assessments of crop production [*Kimetu et al.*, 2008] and soil properties [*Solomon et al.*, 2007] including soil PyC concentrations [*Nguyen et al.*, 2008] in the same region using chronosequences that included a much wider range of sites. Interviews about land use history were supported by local records and our own observations of land use over more than one decade. All headwater catchments are located on similar elevation in close proximity within an area of 6 km^2 (Figure 1) reducing variations in climate, vegetation, or soil type [*Recha et al.*, 2012]. Each headwater catchment has one stream water outlet with no other hydrological input apart from rainfall. Even though the watersheds were carefully selected, variability stemming from factors other than time since forest clearing still remains. Therefore, only clear changes across the entire range of time should be interpreted [*Recha et al.*, 2012, 2013] rather than changes between individual time points.

The forests within the studied catchments are portions of the Kakamega-Nandi forest and are composed of mixed tropical highland species. The tree species are dominated by *Funtumia africana*, *Prunus africana*, *Ficus* spp., *Croton* spp., and *Celtis* spp. [*Glenday*, 2006]. Below and above ground net primary productivity is estimated to be 15.2 Mg ha^{-1} yr^{-1} [*Hertel et al.*, 2009]. The agricultural catchments are complex mosaics of smallholder farming systems dominated by the annual crops of maize (*Zea mays*) and common beans (*Phaseolus vulgaris*) and the perennial crop tea (*Camellia sinensis*) (Figure 2).

In the spring of 2012, the local inhabitants surrounding one of the forest catchments (FA) began the process of felling trees for charcoal production. This continued through late August of 2012. Charcoal production occurred within the catchment in scattered specific locations and was produced using traditional earthen kilns. The large pieces of the finished charcoal were bagged and exported; the fines were left in place.
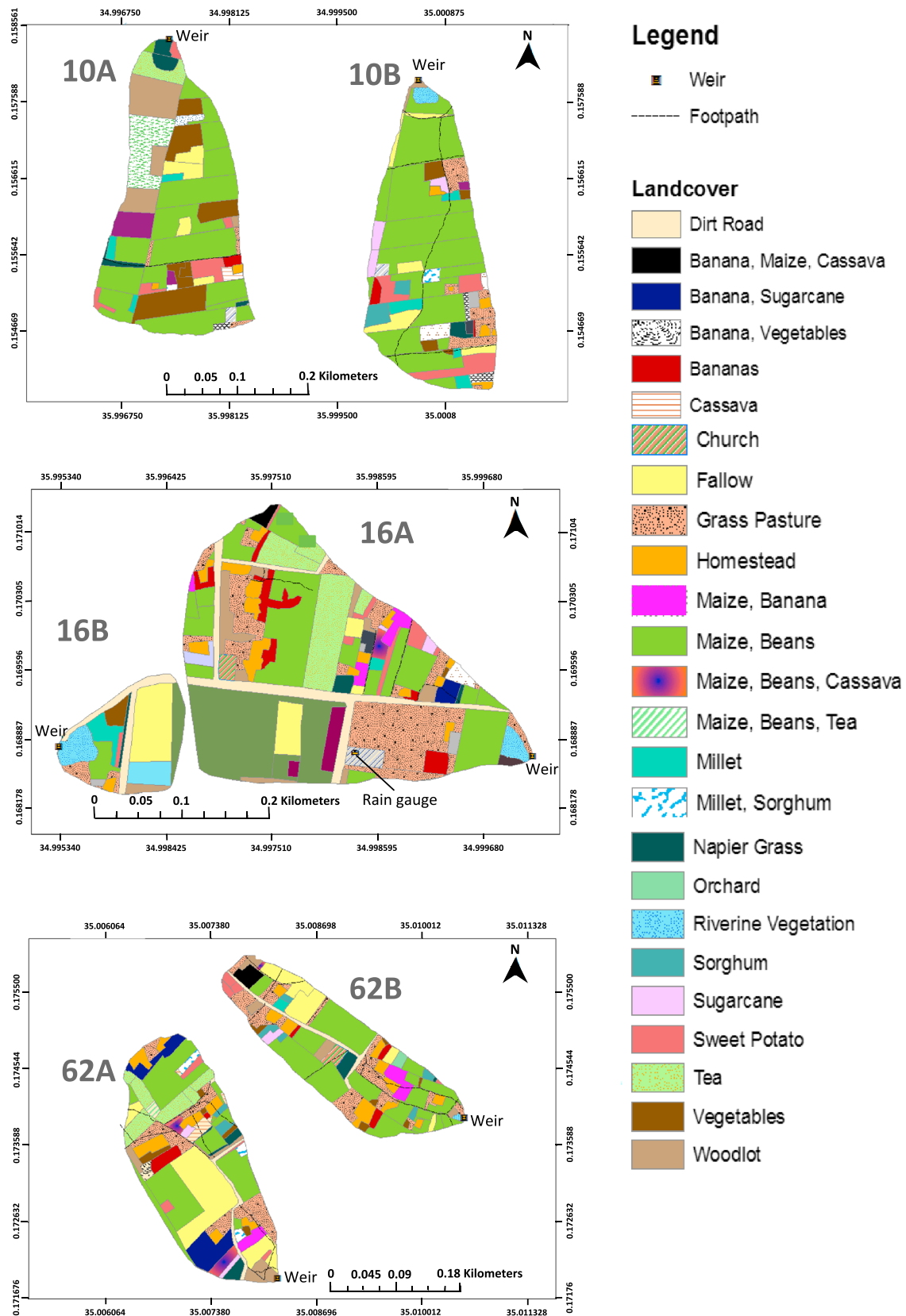
Figure 2. Land use maps of the agricultural catchments in the Kapchorwa region of western Kenya. Data were taken and compiled for the long-rain season of 2013 between June and August 2013. Locations of the weirs are indicated by black diamond boxes.

Table 1. Topsoil (0–0.15 m) Total Organic C (TOC) and PyC Contents and Stocks of Forest (Replicate Catchments FA and FB) and Agricultural Catchments (Replicate Catchments A and B at 10, 16, and 62 years After Burning) in the Kapchorwa Region of Western Kenya[a]

Slope Position (% slope)	TOC (mg g^{-1})	TOC (Mg ha^{-1})	Non-PyC (mg g^{-1})	Non-PyC (Mg ha^{-1})	PyC (mg g^{-1})	PyC (Mg ha^{-1})	PyC (% of TOC)
			Catchment FA				
CH	75.0	90.0	61.5	73.8	13.5 A	16.2 A	17.58 A
<1	69.8	83.8	66.4	79.7	3.4 B	4.1 B	4.98 B
1–3	91.2	109.5	86.1	103.4	5.1 AB	6.1 AB	5.52 B
3–5	72.8	87.4	67.7	81.2	5.1 AB	6.1 AB	7.01 B
5–10	63.5	76.3	56.8	68.1	6.7 AB	9.1 AB	11.67 AB
10–20	72.2	86.6	68.2	81.9	3.9 B	4.7 B	5.63 B
P value	0.4505	0.4505	0.1784	0.1784	0.0016	0.0016	<0.0001
Average	73.8a	88.57a	65.8a	78.94a	8.02a	9.63a	10.95a
			Catchment FB				
<1	73.6 A	88.3 A	71.1 A	85.3 A	2.5 AB	3.00 AB	3.46 B
1 PyC$_{exp}$	56.2 AB	67.4 AB	53.6 ABC	64.4 ABC	2.5 AB	3.1 AB	4.61 AB
1–3	71.6 A	85.9 A	68.0 AB	81.6 AB	3.6 AB	4.3 AB	5.41 AB
1–3 PyC$_{exp}$	64.8 AB	77.7 AB	60.7 ABC	72.9 ABC	4.1 A	4.9 A	6.43 AB
3–5	78.3 A	94.0 A	75.2 A	90.2 A	3.1 AB	3.7 AB	4.10 B
3–5 PyC$_{exp}$	39.1 B	47.0 B	35.5 C	42.6 C	3.6 AB	4.4 AB	9.48 A
5–10	55.4 AB	66.5 AB	52.9 ABC	63.5 ABC	2.5 AB	3.0 AB	4.51 AB
5–10 PyC$_{exp}$	45.7 B	54.8 B	44.2 BC	53.1 BC	1.5 B	1.7 B	3.19 B
P value	0.0003	0.0003	0.0004	0.0004	0.0425	0.0425	0.0115
Average	60.7b	72.90ab	57.9ab	69.50ab	2.84b	3.42b	4.99b
			Catchment 10A				
<1	46.2 AB	63.0 AB	43.0 AB	58.7 AB	3.1 AB	4.3 AB	6.96
1–3	39.8 B	54.3 B	37.7 B	51.5 B	2.1 B	2.8 B	5.44
3–5	59.5 A	81.2 A	55.9 A	76.3 A	3.6 AB	4.9 AB	6.14
5–10	61.3 A	83.6 A	56.5 A	77.1 A	4.8 A	6.6 A	7.87
P value	0.0073	0.0073	0.0127	0.0127	0.0052	0.0052	0.2981
Average	61.7bc	70.54ab	48.3bc	65.87ab	3.42b	4.43b	6.60b
			Catchment 10B				
1	18.2 B	24.8 B	16.9 B	23.0 B	1.3 C	1.8 C	7.31 AB
1–3	29.2 B	39.8 B	26.9 B	36.8 B	2.2 BC	3.0 BC	7.80 A
3–5	65.4 A	89.3 A	61.6 A	84.0 A	3.8 AB	5.2 AB	5.82 AB
5–10	67.0 A	91.5 A	61.9 A	84.5 A	5.1 A	7.0 A	7.53 AB
10–20	59.4 A	81.0 A	55.7 A	76.1 A	3.6 AB	4.9 AB	6.11 AB
20–30	66.7 A	91.0 A	63.3 A	86.4 A	3.4 ABC	4.6 ABC	5.06 B
P value	<0.0001	<0.0001	<0.0001	<0.0001	0.0004	0.0004	0.0207
Average	51.0bc	69.57ab	47.7bc	65.14ab	3.25b	4.67b	6.60b
			Catchment 16A				
<1	56.1	86.8	53.5	82.6	2.7	4.2	4.72
1–3	51.1	79.0	48.3	74.6	2.9	4.5	5.83
3–5	39.2	60.5	36.9	57.1	2.3	3.5	7.11
5–10	40.6	62.7	38.2	59.0	2.4	3.6	5.85
10–20	57.2	88.9	55.3	85.5	2.2	3.4	3.95
P value	0.3712	0.3712	0.3465	0.3465	0.6477	0.6477	0.1991
Average	49.6bc	75.57ab	47.1bc	71.75ab	2.51b	3.82b	5.51b
			Catchment 16B				
<1	57.9	89.5	56.1	86.6	1.8	2.83	3.71
1–3	74.8	115.6	72.7	112.3	2.1	3.26	2.93
3–5	38.4	59.3	36.2	56.0	2.2	3.36	6.36
5–10	37.0	57.2	34.9	54.0	2.1	3.22	6.08
P value	0.1314	0.1314	0.1246	0.1246	0.6948	0.6948	0.0548
Average	45.9bcd	74.06ab	43.9bcd	70.98ab	2.02	3.08b	5.11b
			Catchment 62A				
<1	29.5	51.7	27.2	47.8	2.3	4.0	8.01 AB
1–3	43.1	75.7	40.3	70.7	2.8	5.0	6.98 AB
3–5	36.2	63.4	32.9	57.8	3.2	5.6	8.90 A
5–10	27.7	48.6	25.5	44.8	2.2	3.8	8.11 AB
10–20	31.1	54.6	29.0	50.9	2.1	3.6	6.94 AB
20–30	24.5	41.9	22.9	40.1	1.6	2.9	7.50 AB
>30	33.5	58.8	31.9	55.9	1.6	2.9	4.92 B
P value	0.3987	0.3987	0.4153	0.4153	0.0996	0.0996	0.0683
Average	36.1cd	56.54b	29.9d	52.57b	2.26b	3.97b	7.34b

Table 1. (continued)

Slope Position (% slope)	TOC (mg g⁻¹)	TOC (Mg ha⁻¹)	Non-PyC (mg g⁻¹)	Non-PyC (Mg ha⁻¹)	PyC (mg g⁻¹)	PyC (Mg ha⁻¹)	PyC (% of TOC)
			Catchment 62B				
<1	31.7	55.6	30.0	52.7	1.7	2.9	5.27 B
1–3	25.5	44.8	23.6	41.5	1.9	3.3	7.71 A
3–5	41.2	72.4	38.9	68.2	2.4	4.1	5.75 AB
5–10	41.0	72.0	39.0	68.6	2.0	3.4	4.81 B
10–20	44.2	77.6	42.5	74.6	1.7	3.0	4.06 B
20–30	37.7	66.2	36.2	63.5	1.5	2.7	4.76 B
P value	0.4123	0.4123	0.3958	0.3958	0.0919	0.0919	0.0010
Average	32.2d	63.39b	34.3cd	60.20ab	1.81b	3.19b	5.41b
P value average	<0.0001	0.0002	<0.0001	0.0024	<0.0001	<0.0001	<0.0001

[a]Different letters indicate significant differences; no letters are shown when main effects are not significant. Uppercase letters are used for within-catchment comparisons (Tukey's HSD, $P < 0.05$, $n = 4$, $n = 14$ for CH), lowercase letters are used for between catchment comparisons of spatially weighted average values for all slope positions (Tukey's HSD, $P < 0.05$, $n = 16–140$), and CH represents the charcoal production sites (only in the forest catchment FA). PyC_{exp} (only in the forest catchment FB) indicates data for $1\,m^2$ experimental plots that received $10\,Mg\,ha^{-1}$ charcoal (described in section 2).

There were visibly higher concentrations of charcoal left in these locations after production had finished (Figures S1 and S2 in the supporting information). This land clearing method of "chop and char" is commonly used in the region [*Barnes*, 1990; *Okello et al.*, 2001]. In addition to charcoal production and fire associated with forest clearing for agriculture, anthropogenic and natural fires of forests and grasslands are frequently observed [*Bond et al.*, 2005].

2.2. Soil Sample Collection

Each catchment was divided into distinct slope categories: <1%, 1–3%, 3–5%, 5–10%, 10–20%, and > 20%. The slope categories follow the naturally occurring contours of the catchments. In these landscapes the shallowest slope corresponds to the highest elevation within the landscape and the steepest slope corresponds to the lowest elevation in the landscape. Within each catchment the steepest section of the slope terminates just before the weir with little to no foot slope and is an area of both soil loss and accumulation.

Soil samples were taken from four random locations within each slope-category in each catchment. The randomization of the soil sampling locations was achieved using the Create Random Points function of ArcGIS (ArcGIS 10.1, ESRI, Redlands, California, USA). Samples were taken from four locations in each slope class at depths of 0–0.15, 0.15–0.3, 0.3–0.6, 0.6–1, and 1–2 m using a Dutch-style auger. At each of these four locations, samples were taken in triplicate within an area of $2\,m^2$ and homogenized in a bucket by hand. A 1 kg subsample was then taken from the bucket, air-dried, and sieved through a 2 mm sieve.

At the same locations, runoff and saturated infiltrability were measured using the Cornell Sprinkle Infiltrometer (Cornell University, Ithaca, New York). In addition, saturated infiltrability was measured in all land use units shown in Figure 2. Low-solute water was prepared at the World Agroforestry Centre Kisumu site office using a Thermo Scientific™ Barnstead™ hose nipple cartridge (Thermo Fisher Scientific). The infiltrometers were calibrated to deliver simulated rainfall at a rate of $300\,mm\,h^{-1}$. The rainfall simulation was run for 1 h. Runoff, water, and sediment were collected in 5 L plastic beakers for the different slope positions. Two subsamples of the water and all of the sediment were transferred to individual 50 mL centrifuge tubes (Thermo Fisher Scientific), were preserved by acidifying with 1 drop of concentrated HCl per tube, and then refrigerated.

In June of 2013, locations were identified and mapped where PyC accumulated as a result of charcoal production by the local inhabitants in the forest catchment FA during 2012 (Figures S1 and S2; shown as CH in Table 1). Fourteen individual locations were found each with a spatial extent of about $12\,m^2$. All of these locations were selected for sampling and experimentation which was done randomly within the $12\,m^2$.

In June 2013 small plots with intentional PyC application were established in the FB catchment (shown as PyC_{exp} in Table 1). Charcoal was purchased locally within the catchment villages. This charcoal was produced from a mixture of local forest hardwoods, resembling local practice. The charcoal was pulverized by hand to produce pieces with an average diameter of less than 10 mm. The charcoal was applied in March of 2013 just before the onset of the long rainy season at the equivalent rate of $10\,Mg\,ha^{-1}$ to $1\,m^2$ plots and lightly mixed into the top 0.1 m of the soil using hand hoes. This was intended to simulate the charcoal deposition found in the FA
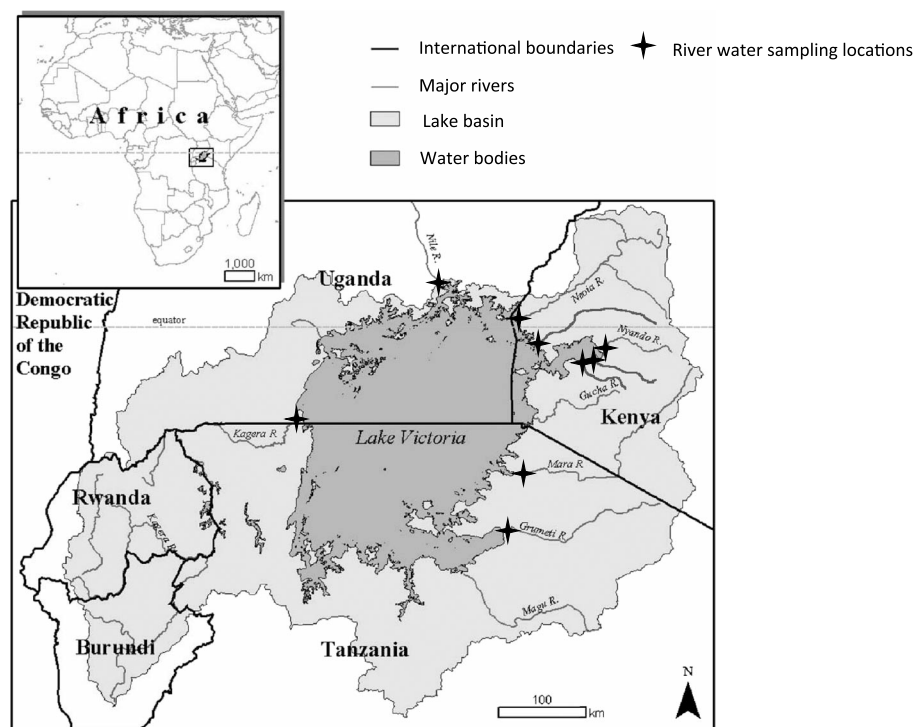
Figure 3. The greater Lake Victoria watershed (adapted from *Albright et al.* [2004]). Location of the Kapchorwa catchments is indicated by the hashed box in the upper right corner of the figure. Approximate locations of river water sampling locations are indicated by large black stars. Approximate locations of lake water sampling sites are indicated by smaller black triangles (coordinates are listed in Table S2 in the supporting information).

catchment. Four of these plots were randomly located within each of the slope-categories within the FB catchment. Soil and runoff samples were taken from both the CH and PyC$_{exp}$ plots as described above.

2.3. Instrumentation, Runoff, and Stream Water Collection

In 2008, hydrological boundaries were established and instrumentation installed. A more detailed description of the setup is given by *Recha et al.* [2012, 2013]. A V notch weir was built at the outlet for each catchment to determine stream discharge. Stream water height was measured using capacitance probes (Odyssey Dataflow Systems Pty Ltd, New Zealand) installed near the weirs. The probes were programmed to give an average reading every 2 min. Data from these probes were downloaded biweekly. Stream hydrographs were normalized by catchment area to allow for comparisons between the different catchments.

Precipitation for the study period was determined by a tipping bucket rain gauge (Rain-O-Matic, Pronamic, RinkØbing, Denmark) connected to a data logger (Hobo® Event Data Logger H07-002-04, Onset Computer Corporation, Bourne, Massachusetts, USA) installed 1 m above the ground. Rainfall for the 1 year study period in the catchment area was 2242 mm, with the greatest rainfall intensity of 136 mm h^{-1}.

Base flow stream water was sampled on a biweekly basis at the water outlet from the weir at the beginning and middle of each month. Forty milliliters of stream water flowing over the weirs were captured directly into 50 mL centrifuge tubes (Thermo Fisher Scientific, Waltham, Massachusetts, USA). Each water sample was preserved by adding 1 drop of concentrated HCl. The samples were then packed into coolers with ice packs and refrigerated.

Water samples were also collected from the outlet of Lake Victoria at Jinja, and all of the major tributaries of this watershed. Sample locations are shown in Figure 3 and Table S2 in the supporting information. River water was sampled on 1 day for each watershed during the rainy season of 2013 between the months of April and June. The rivers were sampled approximately half a kilometer from the point where the river enters the lake in order to obtain a representative upstream sample. River water samples were obtained by filling two 20 L screw cap jugs with water from the top 2 m of the water column in the approximate middle of the river. Prior to filling, the jugs were rinsed with two washes of water from

the respective river. The water from these jugs was homogenized and combined in a single 20 L jug that was also prerinsed with river water. The final jug was filled leaving less than 1% headspace. All of the water samples were preserved by adding 10 mL of concentrated HCl to each 20 L jug. These protocols are similar to *Jaffé et al.* [2013].

2.4. Sample Analysis

One vial of each of the Kapchorwa stream water and runoff samples was filtered through an Advantec® 0.45 μm pore-sized glass fiber filter (Toyo Roshi Kaisha, Ltd., Tokyo, Japan) and the filter as well as dissolved samples was separately processed. The river water samples were not filtered, and only total contents determined. All stream water, river water, and runoff samples (whether filtered, unfiltered, or sediment samples) were freeze-dried (Dura-Dry^{tm} μP, FTS Systems Inc., Stone Ridge, New York).

TOC and PyC were determined for all of the water, soil, and runoff samples using predictions via midinfrared partial least square (PLS) analysis calibrated to hydrogen pyrolysis and dry combustion measurements. The midinfrared spectra for all of the stream water and runoff samples were obtained with a Bruker Tensor Series FT-IR spectrometer (Bruker Optics Inc., Billerica, Massachusetts). The instrument scanning was set to 1 scan s^{-1} for 60 scans with a ZnSe attenuated total reflectance (ATR) objective and DTGS detector. Dry, powdered samples were applied directly to the detector crystal and secured in place with a slight pressure using the ATR clamping utility tool. Spectra were acquired from 8300 to 470 cm^{-1} at a resolution of 8 cm^{-1}. The spectra for the soils were acquired using FTIR spectroscopy from 4000 to 602 cm^{-1} at a resolution of 4 cm^{-1} with a Bruker Optics Tensor 27 (Bruker Optics) attached to a High Throughput Screening eXTension (HTS-XT) unit with a robotic arm (Twister Microplate Handler). Soil samples were finely ground using an agate mortar and pestle and loaded into aluminum microtiter plates (A 752–96, Bruker Optics). Soil samples were then filled into four replicate wells, each well was scanned 32 times, and the four spectra were averaged to account for within sample variability and differences in particle size and packing density. Reference readings were conducted with no sample loaded onto the ATR crystal.

The PLS predictions were generated by calibration to direct TOC and PyC analyses of approximately 10% (152 samples) of the total sample number. The PLS model for PyC and TOC prediction had r^2 values of 0.85 and 0.72, and root mean square errors for the predictions [*Terhoeven-Urselmans et al.*, 2010] of 0.48% and 0.57%, respectively. The samples used for calibration were chosen to represent a broad spectrum of PyC contents to give the PLS model maximum predictive power. Of these subsamples, one sample subset was used to determine total C by Dumas combustion on a Costech ECS 4010 (Costech Analytical Technologies Inc., Valencia, California); since the soils are acidic and the parent material is granite and gneiss, total C is equivalent to total organic C (TOC). PyC was determined by total C quantification using Dumas combustion after hydrogen pyrolysis (hypy) (Strata Technology, Ltd., Middlesex, UK).

The hypy process to determine PyC is described in detail in *Wurster et al.* [2013]. Briefly, subsamples of soil and freeze-dried water samples were loaded with a Mo catalyst using an aqueous/MeOH (1:1) solution of ammonium dioxydithiomolybdate [$(NH_4)_2MoO_2S_2$]. Catalyst weight was approximately 10% of the sample weight, to give a nominal loading of 1% Mo. Catalyst-loaded samples were lyophilized and placed in the hypy reactor, pressurized with H_2 to 15 MPa with a sweep gas flow of 5 L min^{-1}, then heated using a preprogrammed temperature profile. We used the recommended temperature program previously optimized for PyC quantification, where samples are initially heated at 300°C min^{-1} to 250°C and then at 8°C min^{-1} to 550°C (2 min dwell) [*Ascough et al.*, 2009; *Meredith et al.*, 2012].

2.5. Calculation of Stream PyC and TOC Export

In the Kapchorwa catchments cumulative stream discharge was calculated from stream height for the same two-week intervals that the stream water was sampled [*Recha et al.*, 2012, 2013]. The stream base flow PyC and TOC concentrations were multiplied by the corresponding cumulative discharge for the same 2 week period to obtain total stream export of PyC and TOC. This biweekly export was then used to estimate total annual PyC and TOC exports for the period from mid-August 2012 to mid-August 2013. Missing values due to loss of samples were linearly interpolated. Samples taken during base flow in these watersheds were found to be representative of storm flow concentrations and base flow accounted for 70 to 80% of total discharge [*Recha*, 2011; *Recha et al.*, 2012].
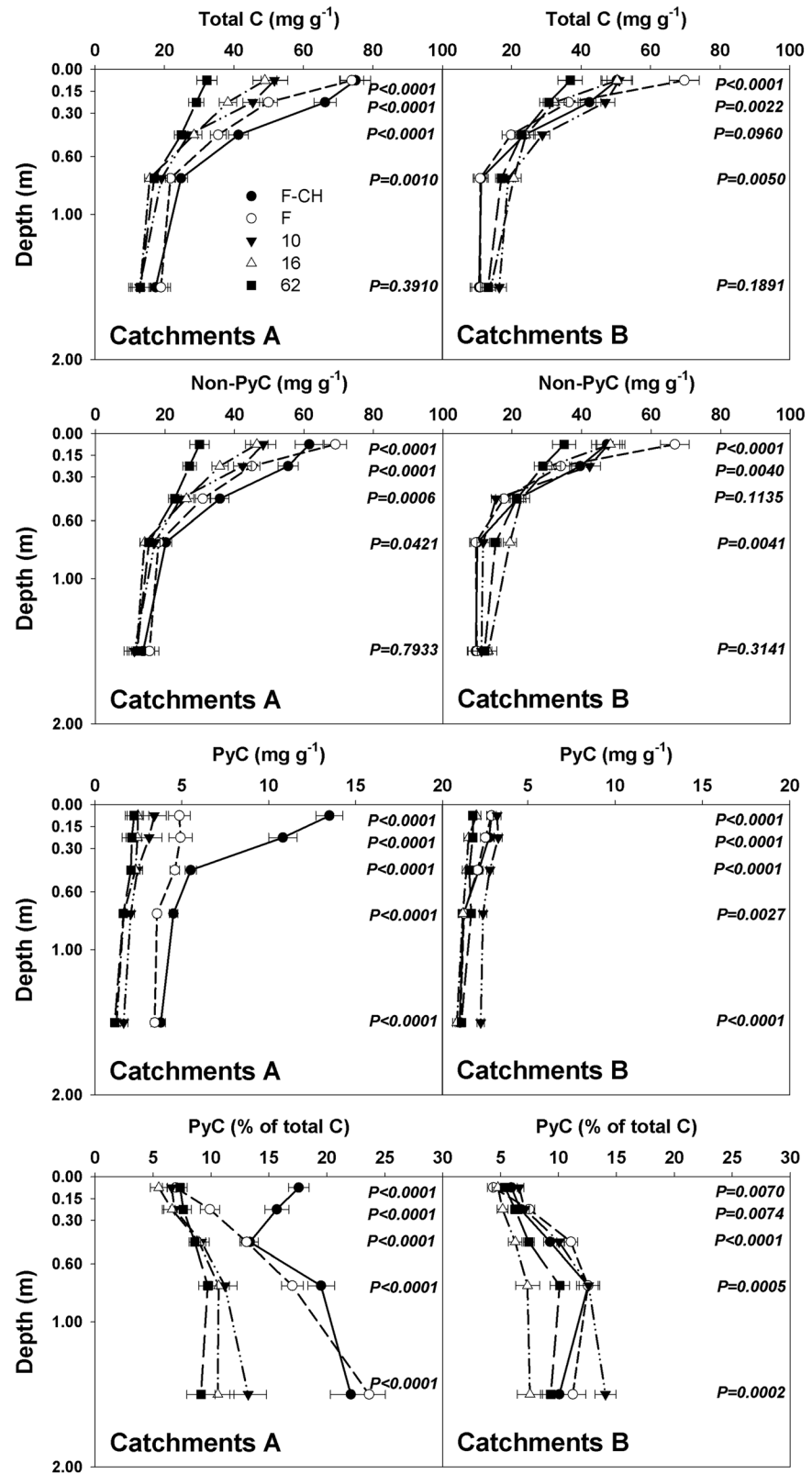
Figure 4. Soil profile total C and PyC of forest and agricultural catchments in the Kapchorwa region of western Kenya. Statistical significance from each depth is indicated by the corresponding *P* value (Tukey's HSD, *P* < 0.05, FA *n* = 36, FB *n* = 48, 10A *n* = 25, 10B *n* = 36, 16A *n* = 30, 16B *n* = 24, 62A *n* = 42, and 62B *n* = 36 for averages of all slope positions). F-CH is the charcoal production site data from forest catchment FA (*n=14*) (left side are catchments A, right catchments B).
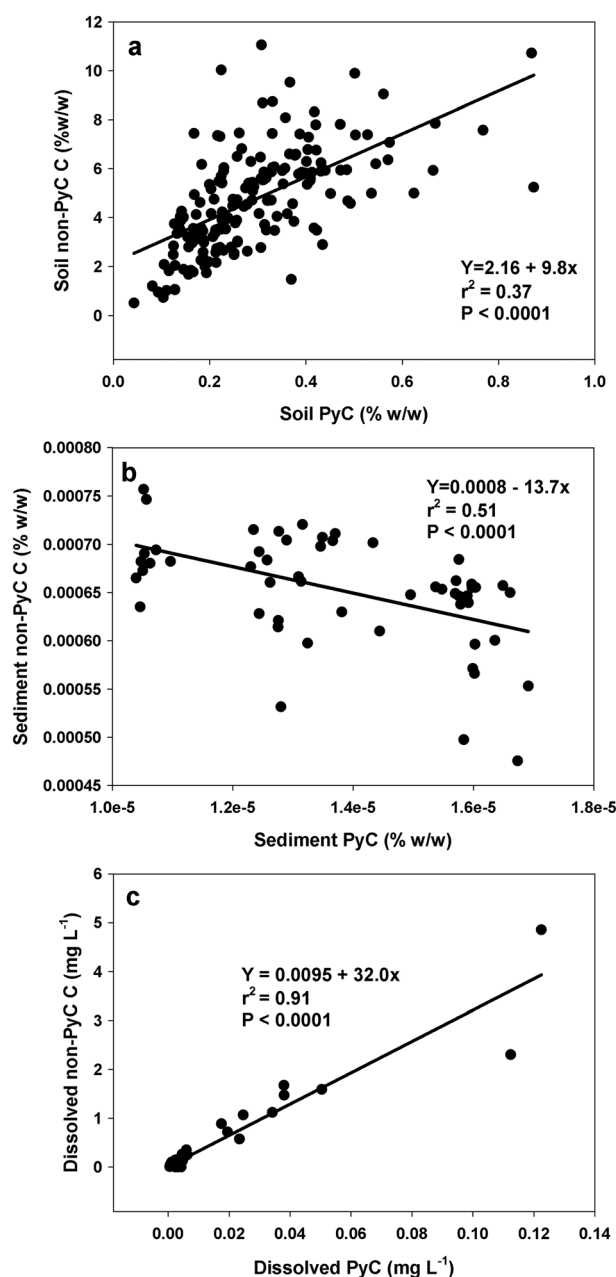
Figure 5. Linear correlations of the concentrations of PyC and non-PyC in (a) soil (0–0.15 m) ($n = 180$), (b) sediment ($n = 57$), and (c) dissolved organic matter of stream water ($n = 89$). Solid lines are the regression lines of the data points that correspond to the accompanying equations, Pearson correlation coefficients, and P values.

Average annual discharge for rivers in the greater Lake Victoria watershed was taken from the literature. Estimated annual export of TOC and PyC was calculated by multiplying the concentrations from the sampled stream water by the published annual discharge. Our detailed assessments of the Kapchorwa headwater catchments showed negligible variation of stream water TOC [*Recha et al.*, 2013] and PyC concentrations (this study) throughout the year. We therefore assumed that the temporal dynamics of PyC concentrations in the rivers around Lake Victoria were also unrelated to the amount of base flow discharge as shown for solutes in Kapchorwa [*Recha et al.*, 2013]. The calculated annual PyC export for the larger rivers in the Lake Victoria watershed have to be taken with caution and provide only a starting point for further inquiry.

2.6. Statistical Analysis

Linear regression, analysis of variance, and mean separation were performed with JMP software (SAS, Cary, North Carolina). Kriging analysis was performed with ArcGIS 10 (ESRI, Redlands, California). All procedures were performed at $P < 0.05$, unless otherwise indicated. Significant treatment effects were determined using the Tukey's honest significant difference (HSD) test.

3. Results

3.1. Soil Depth Profiles

Within the top 0.15 m of soil, TOC concentrations averaged across all slope positions decreased from about 75 mg g^{-1} in the forested catchments to 30 mg g^{-1} in the oldest agricultural catchments (Figure 4). In all of the catchments, TOC concentrations decreased to 10 mg g^{-1} at a depth of 1–2 m.

Average topsoil PyC concentrations (0–0.15 m) were greatest, 14 mg g^{-1}, at the charcoal production sites (CH, charcoal production sites were only found in the forest catchment FA) compared to 4 mg g^{-1} outside those sites (Figure 4). Topsoil and subsoil PyC concentrations averaged for the entire watersheds did not systematically change from forest to agricultural soils.

Soil PyC was enriched with depth in relation to other SOC. The proportion of PyC in TOC increased from 4 to 7% at a depth of 0–0.15 m to 12–24% at 1–2 m in the two forest catchments, and from 5 to 7% at a depth of 0–0.15 m to 8–14% at 1–2 m in the agricultural catchments (Figure 4). In the topsoil of the FA

Table 2. Total Organic C and PyC Contents Captured in Water and Sediment Runoff From Infiltrometer Plots of Forest (Replicate Catchments FA and FB) and Agricultural Catchments (Replicate Catchments A and B at 10, 16, and 62 years After Burning) in the Kapchorwa Region of Western Kenya[a]

Site	TOC[b] (mg L^{-1})	PyC[b] (mg L^{-1})	PyC (% of TOC)	DOC Tot (mg L^{-1})	DPyC (mg L^{-1})	DPyC (% DOC Tot)	TOC (g ha^{-1})	PyC (g ha^{-1})	DOC Tot (g ha^{-1})	DPyC (g ha^{-1})	Sediment TOC (mg g^{-1})	Sediment PyC (mg g^{-1})	Sediment PyC (% TOC)
FA	0.152	0.003	1.3	0.148	0.003	1.8	580	7.63	535	9.60	0.063	0.001	1.3
FB	0.125	0.003	2.4	0.104	0.002	1.7	318	7.06	274	4.85	0.004	0.000	2.4
FB-PyC$_{exp}$	0.179	0.003	2.0	0.204	0.003	1.7	422	8.54	542	7.06	0.077	0.002	2.0
10A	NR	NR	NR	NR	NR	NR	NR	NR	NR	NR	NR	NR	NR
10B	0.168	0.002	1.6	0.139	0.003	2.2	412	6.22	325	7.03	0.175	0.003	1.6
16A	0.166	0.003	1.8	0.182	0.004	1.9	390	6.86	446	8.45	0.668	0.016	1.8
16B	0.163	0.003	1.8	0.157	0.003	1.9	457	8.02	437	8.42	0.063	0.002	1.8
62A	0.167	0.003	1.8	0.154	0.003	2.1	361	6.43	332	6.64	0.577	0.010	1.8
62B	0.130	0.003	1.8	0.138	0.003	1.7	270	4.70	308	5.27	0.063	0.001	1.8
P value	0.4331	0.3411	0.5493	0.2926	0.3652	0.8160	0.3137	0.2902	0.4223	0.5397	0.9086	0.8254	0.5493

[a]Different letters indicate significant differences; no letters are shown when main effect is not significant (Tukey's HSD, $P < 0.05$, FA $n = 36$, FB $n = 48$, 10A $n = 25$, 10B $n = 36$, 16A $n = 30$, 16B $n = 24$, 62A $n = 42$, 62B $n = 36$). FB-PyC$_{exp}$ (only in the forest catchment FB) indicates data for 1 m^2 experimental plots that received 10 Mg ha^{-1} charcoal (described in section 2). No runoff (NR) was captured in the catchment 10A.
[b]Flow-weighted averages.

charcoal production sites (CH) PyC was enriched to a greater extent (18% of TOC) relative to the noncharcoal production sites (7%) or the agricultural catchments (5–7%). Topsoil PyC and non-PyC were weakly but significantly correlated ($r^2 = 0.37$, $P < 0.0001$; Figure 5a).

3.2. Topsoil Catena

Within the forest catchment FA no systematic differences were observed in the investigated topsoil (0–0.15 m, unless indicated otherwise) PyC or TOC contents as a function of slope (Table 1; for maps see Figures S3 and S4 in the supporting information). Despite intentional additions of 10 Mg ha^{-1} charcoal to small experimental plots of 1 m^2 in the forest catchment FB, total PyC did not change measurably in those plots at any of the slope positions (marked with "PyC$_{exp}$" in Table 1). After 10 years of continuous cultivation topsoil stocks of TOC, non-PyC, and PyC were 30, 32, and 50% greater in lower (with greater slope) than higher (with less slope) landscape positions in catchment 10A and 264, 274, and 280% in catchment 10B, respectively (Table 1). Over time, the landscape distribution of PyC reversed and topsoil PyC stocks were slightly greater at higher landscape positions ($P < 0.1$; Table 1). Sixty-two years after forest clearing by fire, the proportion of topsoil PyC in TOC was 80–90% greater in higher landscape positions relative to the lower positions, and average PyC proportions were 7.7% of TOC (ranging from 3% to 11% weighted average for each watershed).

3.3. Rainfall Experiments

Concentrations and fluxes of PyC, non-PyC, or TOC in dissolved organic matter or sediments of runoff induced by experimental rainfall were not significantly different between any of the catchments (Table 2). No correlation was found between PyC in the soil and the sediment captured in the induced water erosion ($r^2 = 0.04$; $P = 0.14$; Figure 6a); neither with total ($r^2 = 0.28$) or dissolved ($r^2 = 0.17$) PyC (data not shown). The PyC values in runoff sediments (Table 2) were two orders of magnitude lower than those found in the soils (Table 1). Infiltrability was not significantly different between chronosequence ages or slope positions but higher at locations with charcoal production and lower at locations of high foot traffic (Tables S3–S5 in the supporting information).

3.4. Stream Water TOC and PyC Concentrations

TOC concentrations in the stream water base flow were greater in the medium and old agricultural catchments then in the forest or young agricultural catchments (Table 3; Figure S5 in
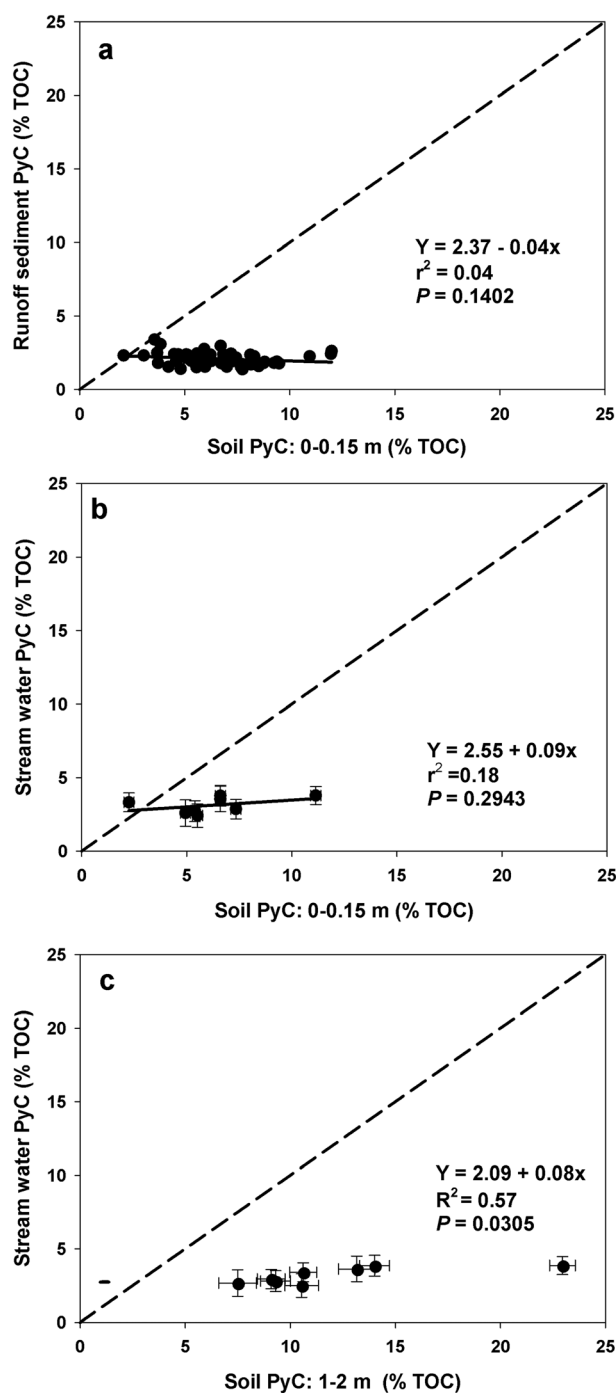
Figure 6. Linear correlations between (a) soil PyC (% TOC) (0–0.15 m) and runoff sediment PyC (% TOC) ($n = 57$), (b) soil PyC (% TOC) (0–0.15 m) and stream water PyC (% TOC) ($n = 8$), and (c) soil PyC (% TOC) (1–2 m) and stream water PyC (% TOC) ($n = 8$). Hashed line represents a 1:1 relationship. Solid lines are the regression lines of the data points that correspond to the accompanying equations, Pearson correlation coefficients, and P values (number of measurements for standard error bars: (a) $n = 1$, and (b) $n = 24$–48 for soil data (from Figure 4) and (c) $n = 24$ for stream water PyC (from Figure S6 in the supporting information); error bars may be smaller than symbols).

the supporting information). In contrast, there were no obvious trends in base flow PyC concentrations between any of the catchments (Table 3; Figure S6 in the supporting information). Neither TOC nor PyC concentrations varied between seasons despite episodic changes in stream water discharge (Figures S5 and S6 in the supporting information). Stream water PyC and non-PyC concentrations were highly correlated for dissolved species ($r^2 = 0.91$, $P < 0.0001$; Figure 5c), whereas this was not the case for sediments ($r^2 = 0.37$, $P < 0.0001$; Figure 5b). Base flow stream water PyC concentrations as a fraction of TOC were not related to the PyC concentrations in the top soil (0–0.15 m) ($r^2 = 0.18$, $P = 0.2943$; Figure 6b). However, base flow stream water PyC concentrations were correlated to soil PyC concentrations in the 1–2 m portion of the soil column ($r^2 = 0.57$, $P = 0.0305$; Figure 6c).

3.5. Annual TOC and PyC Exports

On average, annual exports of PyC (as determined by hydrogen pyrolysis and midinfrared spectroscopy) by stream water were 2 orders of magnitude smaller than TOC exports (Table 3). Annual stream water TOC and PyC exports were 1 order of magnitude lower in the forest than the agricultural catchments, whereas the proportion of PyC in TOC was greater in the forested catchments than in most of the agricultural catchments. The differences in solute export of TOC and PyC between watersheds were a result of both different discharge as well as different TOC and PyC concentrations (Table 3).

Estimated exports of TOC and total PyC (including both dissolved and sediment C) from the major rivers flowing into and out of Lake Victoria, when normalized by catchment area, were approximately 2 orders of magnitude greater than the exports from the Kapchorwa catchments (Table 4). Estimated PyC exports ranged from 0.12 kg ha^{-1} yr^{-1} leaving Lake Victoria through the River Nile (the White Nile) at Jinja, Uganda, to 6.5 kg ha^{-1} yr^{-1} leaving the Gucha River in Kenya, albeit with very limited

Table 3. Concentrations (Flow-Weighted Averages for Each Watershed; Standard Errors are Shown in Figure 6b), Annual Stream Water Discharge, and Annual Amounts of TOC and PyC (Sum of Sediment and Dissolved Species) As Well As Dissolved Species Leaving Forest (Replicate Catchments FA and FB) and Agricultural Catchments (Replicate Catchments A and B at 10, 16, and 62 years After Burning) in the Kapchorwa Region of Western Kenya (Biweekly Data of Concentrations are Shown in Figures S6 and 7 in the Supporting Information) (SE Standard Error of the Averages of all Eight Watersheds (Except for Discharge))

Site	TOC ($mg\,L^{-1}$)	PyC ($mg\,L^{-1}$)	Discharge ($mm\,yr^{-1}$)	TOC ($kg\,ha^{-1}\,yr^{-1}$)	PyC ($kg\,ha^{-1}\,yr^{-1}$)	PyC (% TOC)	DOC Tot ($kg\,ha^{-1}\,yr^{-1}$)	DPyC ($kg\,ha^{-1}\,yr^{-1}$)	DPyC (% DOC Tot)
FA	0.14	0.004	198	0.35	0.010	2.9	0.46	0.015	3.3
FB	0.05	0.001	445	0.21	0.006	2.9	0.19	0.012	6.3
10A	0.35	0.009	365	1.23	0.033	2.7	0.17	0.006	3.5
10B	0.32	0.012	535	1.47	0.056	3.8	0.27	0.010	3.7
16A	0.18	0.004	318	0.55	0.012	2.2	0.17	0.005	2.9
16B	0.09	0.002	2681[a]	2.47	0.056	2.3	2.01	0.058	2.9
62A	0.18	0.004	714	1.06	0.022	2.1	0.50	0.015	3.0
62B	0.13	0.003	663	0.86	0.020	2.3	0.66	0.041	6.2
Average	0.18	0.005	463	0.82	0.023	2.6	0.35	0.015	3.9
±SE	0.04	0.001	66	0.17	0.006	0.2	0.07	0.004	0.5

[a]High discharge values due to the presence of a school in watershed; calculated averages of export do not include values from this watershed.

sampling intensity. In contrast, the proportion of PyC to TOC from these rivers covers, with 1–9% (flow-weighted average of $4.9 \pm 0.8\%$), a similar range to what was measured in the Kapchorwa catchments with 1–10% (flow-weighted average of $2.7 \pm 0.2\%$). The range of values covers the concentration that was measured at the outlet of Lake Victoria into the White Nile (1.1%).

4. Discussion

4.1. PyC Deposition

Charcoal production and PyC deposition was observed to occur in concentrated locations throughout the forested catchment (FA) (Figures S1 and S2 in the supporting information; Table 1 and Figure 4) rather than as a uniform deposition. This pattern is supported by other observations in similar forest systems in Africa [*Bleher et al.*, 2006; *Geist and Lambin*, 2002; *Müller and Mburu*, 2009]. Some of the PyC produced by forest conversion was certainly exported to the atmosphere during production but was considered to be of minor importance compared to short-range deposition to soil [*Bird et al.*, 2015]. The PyC contents existing prior to forest clearing of $6\,Mg\,ha^{-1}$ can be explained by fires that are part of the natural ecology of forests in this region [*Tsingalia and Kassily,* 2009].

4.2. Export and Horizontal Redistribution of PyC Within Catchments

Sixty-two years after initial forest clearing topsoil PyC stocks had decreased by 20–59% (calculated from Table 1). The disappearance of topsoil PyC at the catchment scale was greatest in approximately the first two decades after forest clearing and deposition, after which the PyC stocks remained unchanged. This mirrors conclusions by *Nguyen et al.* [2008] from plot-scale studies in the same region. If this decrease is mostly attributed to physical loss, its magnitude compares favorably with estimated physical losses of 20–53% of char-C applied to experimental plots [*Major et al.*, 2010]. However, the erosion losses shown by *Major et al.* [2010] already occurred over the first 2 years after application.

The slower decreases in soil PyC stocks in our study than those shown by *Major et al.* [2010] may be explained by redistribution through deposition of eroded PyC within the headwater itself. Before the fire clearing, topsoil PyC (0–0.15 m) was evenly distributed in the forest catchments (Table 1; Figure S3 in the supporting information; apart from localized accumulation in charcoal production sites CH in catchment FA). Ten years after forest clearing, there were clear indications of PyC redistribution across the landscape ($P < 0.05$). Between 1.0 and $1.6\,Mg\,ha^{-1}$, 66 and 74% of the topsoil PyC, was lost from areas upslope with an accumulation of 1.9 and $2.9\,Mg\,ha^{-1}$ in areas downslope. These PyC decreases upslope would be interpreted as a loss in plot-scale studies. Physical movement likely accounts for most of these differences in PyC, as differential mineralization [*Lehmann et al.*, 2015] or deposition by fire in situ (from crop residues) is not likely to result in such clear changes across the landscape over a relatively short period of time.

4.3. Vertical Redistribution of PyC

Vertical redistribution of PyC in the soil must also have occurred, since PyC was significantly enriched with depth in comparison to non-PyC. In the topsoil (0–0.15 m) the proportion of PyC to TOC ranged

from 5 to 11% (excluding the sites where charcoal production occurred). At 1–2 m within the soil profile, this concentration increased to between 9 and 13% in the agricultural catchments and to between 22 and 24% in the forest catchments. Similar to the topsoil PyC concentrations, also the concentrations of subsoil (1–2 m) PyC significantly ($P < 0.001$) decreased over the course of the chronosequence. This points at movement of PyC through the subsoil as a relevant mechanism for the disappearance of PyC from terrestrial ecosystems.

Several studies have documented the downward movement of PyC in the soil profile [*Brodowski et al.*, 2007; *Leifeld et al.*, 2007; *Major et al.*, 2010]. Both *Leifeld et al.* [2007] and *Dai et al.* [2005] reported greater proportions of PyC as a fraction of TOC deeper in the soil profile. This suggests that either a preferential movement of PyC down the soil profile (exceeding any direct deposition of non-PyC by plant roots) or greater persistence compared to non-PyC within deeper parts of the soil profile or during transport. Our data do not allow us to conclude which process occurred.

Movement into the subsoil can be a result of leaching with percolating water or bioturbation, and evidence for both has been found in previous studies. *Leifeld et al.* [2007] calculated significant PyC transport rates of 6–12 mm yr^{-1} in peat soil through analyses of soil profiles. In contrast, *Major et al.* [2010] measured leaching of applied PyC over the course of 2 years using free-draining lysimeters and documented that only 0.02% of the applied PyC moved below 0.3 m with percolating soil water. It is not known whether this movement in soil water will continue at such a low rate but suggested a minor flux by leaching even over decadal and centennial time scales [*Foereid et al.*, 2011]. Different soil properties at our site may influence the percolation and retention of PyC. Another potential mechanism for vertical translocation of PyC is movement via bioturbation. In temperate environments earthworms are known to play an important role in SOC cycling to depth. In tropical Africa, termites are a major constituent of soil mesofauna and play a dominant role in the cycling of SOC [*Bignell et al.*, 1997; *Bonachela et al.*, 2015; *Jones*, 1990]. In the process the associated bacteria in the termites digestive system [*Breznak*, 2000] may metabolize the non-PyC to a greater extent than the PyC, which may contribute to the enrichment of PyC with depth.

4.4. Export Pathways of PyC From Headwaters and Implications for Global PyC Cycles

Several lines of evidence point to a significant contribution of subsurface PyC to stream export and input to major rivers. The relationship between PyC concentrations in the stream water to the PyC concentrations at a depth of 1–2 m but not the top 0.15 m (Figures 6b and 6c) suggests that a significant portion of PyC exported by streams during base flow originates from the subsoil. This is supported by the enrichment of PyC in TOC in the subsoil and the disappearance of PyC in the subsoil over time (Figure 4).

It is possible that PyC accounting has largely overlooked the contributions of subsoil PyC to the global biogeochemical PyC cycles. In the data presented here PyC correlated well with non-PyC during the investigated base flow (Figure 5c) which constitutes the majority of stream discharge [*Recha et al.*, 2012]. If subsurface transport pathways largely dominate PyC movement from terrestrial to aquatic systems, this might be a potential explanation for the suggested coupling of PyC and DOC proposed by *Jaffé et al.* [2013] for global fluvial systems. The lack of a positive relationship between PyC and non-PyC in stream sediment export (Figure 5b), more likely to have originated from eroded topsoil than the subsoil as known for leaf litter fragments [*Johnson et al.*, 2006], also points at the subsoil source as a more likely reason for this coupling. While previous studies have shown erosion as a major mechanism for PyC movement from soil [*Rumpel et al.*, 2006a; *Major et al.*, 2010; *Dittmar et al.*, 2012], our study shows that subsurface processes provide the bulk of the PyC input to streams and erosion may be more important in redistribution of PyC between slope positions as discussed above.

At the larger scale of the rivers entering and leaving Lake Victoria additional mobilization processes are likely at play in comparison to the headwaters, for which we do not find preferential mobilization of either PyC or non-PyC. The one hundredfold increase in absolute TOC and PyC concentrations and exports with greater catchment size may have several reasons: (i) erosion may play a larger role at larger scales; (ii) losses from the investigated headwaters are lower than from lower lying areas that are usually more densely populated; and/or (iii) mobilization of bank sediments occurred during the rainy season. These spatial dynamics in upstream and downstream solute transport have been documented in previous studies of other large watersheds [*Walling and Webb*, 1980]. The similar proportion of PyC, 1–10% of TOC, may suggest certain similarities in behavior of PyC and non-PyC across scales.

Table 4. Total C and PyC Concentrations, Stocks, and Estimated Annual Exports in the Greater Lake Victoria Watershed, Headwaters of the White Nile

Site	Native Ecological Zone	Catchment Area (km²)	Average Annual Discharge (m³ s⁻¹)	TOC (mg L⁻¹)	PyC (mg L⁻¹)	PyC (% Total C)	TOC (kg ha⁻¹ yr⁻¹)	PyC (kg ha⁻¹ yr⁻¹)	TOC (Gg yr⁻¹)	PyC (Gg yr⁻¹)
R. Yala	Highland forest	3,240	27[a]	13.5	0.5	3.7	36	1.25	11.5	0.4
R. Nzoia	Highland forest	12,900	118[a]	14.0	0.7	5.0	40	1.88	52.0	2.4
R. Nyando	Savannah	3,500	13[c]	20.3	1.6	7.9	24	1.84	8.3	0.6
R. Awach	Savannah	1,985	4[a]	10.3	0.5	4.9	7	0.34	1.3	0.1
R. Sondu-Miriu	Savannah	3,470	45[c]	7.8	0.3	3.8	32	1.34	11.0	0.5
R. Gucha	Highland forest	6,600	66[c]	23.6	2.1	8.9	74	6.52	49.1	4.0
R. Kibuon	Highland forest	760	6[c]	10.5	0.7	6.7	26	1.78	2.0	0.1
R. Simiyu	Savannah	5,320	30[e]	11.8	0.4	3.4	21	0.74	11.1	0.4
R. Kagera	Highland forest	60,000	184[d]	23.9	0.4	1.7	23	0.36	138.8	2.2
R. Mara	Savannah	13,504	35[b]	9.7	0.2	2.1	8	0.18	10.7	0.3
R. Nile at Jinia	Lake Victoria	238,900	981[f]	8.1	0.1	1.1	11	0.12	250.0	2.8

[a]Sangale et al. [2012].
[b]Mutie et al. [2006].
[c]Okungu and Opango [2012].
[d]Food and Agricultural Organization [2014].
[e]Rwetabula et al. [2007].
[f]Ahmed and Ismail [2008].

4.5. Dynamics of PyC and Non-PyC Movement
4.5.1. Differential Movement of PyC and Non-PyC

We hypothesized that PyC movement and loss will be preferential to non-PyC movement. This hypothesis was based on previous studies that found preferential PyC movement from plot studies [*Rumpel et al.*, 2006a, 2006b], from headwater studies [*Guggenberger et al.* 2008], and from large watersheds [*Jaffé et al.*, 2013]. In this study we did not find preferential PyC movement. In contrast, we found preferential movement of non-PyC.

Assuming that preferential erosion of PyC occurred, we would expect to see a greater depletion of PyC than TOC in the upper slope positions and corresponding enrichment in the lower slope positions over time. Our data indicate the opposite; after a decrease of both TOC and PyC upslope and increase downslope, there is an upslope enrichment of PyC in TOC in the topsoils 16 and 62 years after forest clearing (Table 1 and Figures S3 and S4 in the supporting information). This could be explained by lower movement and/or greater persistence of PyC compared to other forms of SOC [*Cheng et al.*, 2008; *Liang et al.*, 2008]. Preferential movement of PyC cannot explain this landscape-scale distribution.

Direct experimental evidence against preferential erosion of PyC at our sites is shown by the runoff data. Surficial water and TOC flow could for the most part be initiated with simulated rainfall events only if it exceeded saturated conductivity such as in high-traffic turf, roads, and woodlots (Table S5 in the supporting information) and infiltrability significantly increased at locations of charcoal production (Table S4 in the supporting information). The calibrated simulated rainfall required to induce runoff was 300 mm h⁻¹, which was well above the maximum rainfall intensity of 136 mm h⁻¹ found for the measurement period. Therefore, significant erosion of any OC may rarely occur

in forests and crop fields within the study sites. This lack of saturation excess runoff is typical for deep and highly weathered soils with high permeability [*Mbagwu*, 1997; *Renck and Lehmann*, 2004].

When erosional events were induced with the infiltrometer and the sediments were captured, no increases in PyC concentration as a proportion of TOC were observed in the runoff over time. Additionally, the PyC concentration in the runoff was not greater relative to the soil that the runoff-TOC originated from. This was true even in the forest plots (PyC$_{exp}$) where fresh PyC was added to experimental plots as well as at the slightly larger scale of entire headwater catchments. Therefore, PyC was not preferentially transported within and from the studied headwaters.

4.5.2. Reasons for Lack of Preferential PyC Movement From Headwaters to Regions

Differences in deposition and therefore distribution of PyC above and below ground may be one reason for the differences in PyC and non-PyC export seen in our study compared to other studies at similar scale [*Rumpel et al.*, 2006a, 2006b; *Guggenberger et al.*, 2008]. During natural forest fire or slash and burn events much of the aboveground non-PyC would be volatilized through burning or be converted to PyC. In this scenario PyC would be the dominant OC species deposited onto the soil surface and would therefore be the predominant OC form exposed to erosional forces. This is likely the scenario reported in *Rumpel et al.* [2006a]. Hence, rather than preferential erosion of PyC, a greater proportion of PyC export may be explained by the fact that the non-PyC stocks on the topsoil would be reduced due to the fire event. In addition, PyC would be deposited on the topsoil or remain on remnants of vegetation [*Schmidt*, 2004] instead of being incorporated into the soil. PyC would thereby erode preferentially by virtue of its location on or above the soil surface rather than for reasons of its material properties.

The lack of preferential erosion of PyC and rather a preferential erosion of non-PyC measured in our study even immediately after PyC deposition may possibly be explained by the incorporation of the PyC into the soil, as would occur during the land use change simulated here, which resembles chop and char rather than slash and burn. The relationship between the PyC fraction in both the eroded sediment as well as the stream water and soil (Figure 5) always remained below a 1:1 line regardless of site history. This suggests that additional mechanisms may be responsible for a proportionally greater retention of PyC within the landscape. A lower movement of PyC than non-PyC may be explained by interactions of PyC with minerals [*Brodowski et al.*, 2006; *Liang et al.*, 2008] that could reduce mobility. These multiple lines of evidence further strengthen the argument that PyC was not preferentially eroded in comparison to non-PyC in the studied watersheds. On the contrary, the data imply that PyC might be retained to a greater extent than non-PyC.

In addition, the proportion of PyC to TOC leaving the Yala River flowing into Lake Victoria (3.5%) is similar to the average value from the Kapchorwa catchments (2.6 ± 0.2%), headwaters of the Yala River. These data suggest that the relationship between the export of PyC and TOC shown for the Kapchorwa catchments is similar across the entire Yala River catchment, despite what are likely different fire events and vegetation. For the main rivers of the entire Lake Victoria watershed, the magnitude of this relationship remains similar (4.9 ± 0.8% weighted average of all 10 major rivers) despite large changes in the export stocks of TOC and PyC between the constituent river systems. Processes found at the Kapchorwa catchments such as PyC redistribution within the watershed and the dominant contribution of subsurface PyC to stream water may therefore be typical for fire-prone East African landscapes and possibly other regions where vegetation is cleared by fire. This contrasts with PyC assessments in the Paraiba do Sul River of Brazil where subsurface PyC sources were found to be less important than erosion [*Dittmar et al.*, 2012].

5. Conclusion

Our data suggest that the movement of PyC is not greater but even proportionally lower than that of non-PyC in the studied catchments. The driving mechanisms behind this greater retention of PyC are unclear and may include adsorption to mineral particles but warrant further investigations. We estimate the yearly PyC input into Lake Victoria from its major tributaries at 11 Gg yr^{-1} and input into the upper White Nile from Lake Victoria at 2.8 Gg yr^{-1} (as quantified by hydrogen pyrolysis and midinfrared spectroscopy). The data in this paper suggest that subsurface flow rather than erosion may govern this large movement of PyC from terrestrial to aquatic ecosystems. Movement of PyC and non-PyC through subsurface flow paths may provide a reason for their coupling observed in global rivers, but this will need to be verified for other regions. Our data may also suggest that large-scale applications of anthropogenic PyC across similar landscapes may not

necessarily result in preferential transport losses of applied-PyC. Further research is needed to verify the results from this study for other catchments. In addition, intensive monitoring of catchment-scale experimental applications of PyC over multiple years will be needed to quantify the contributions of mineralization and erosional losses of PyC over time.

References

Ahmed, A. A., and U. Ismail (2008), *Sediment in the Nile River System*, United Nations, Khartoum, Sudan.

Albright, T. P., T. Moorhouse, and T. McNabb (2004), The rise and fall of water hyacinth in Lake Victoria and the Kagera River Basin, 1989–2001, *J. Aquat. Plant Manage.*, *42*, 73–84.

Alexis, M. A., D. P. Rasse, H. Knicker, C. Anquetile, and C. Rumpel (2012), Evolution of soil organic matter after prescribed fire: A 20-year chronosequence, *Geoderma*, *189*, 98–107.

Ascough, P. L., M. I. Bird, F. Brock, T. F. G. Higham, W. Meridith, C. E. Snape, and C. H. Vane (2009), Hydropyrolysis as a new tool for radiocarbon pre-treatment and the quantification of black carbon, *Quat. Geochronol.*, *4*, 140–147. Barnes, R. (1990), Deforestation trends in tropical Africa, *Afr. J. Ecol.*, *28*, 161–173.

Bignell, D. E., P. Eggleton, L. Nunes, and K. L. Thomas (1997), Termites as mediators of carbon fluxes in tropical forest: Budgets for carbon dioxide and methane emissions, in *Forests and Insects*, edited by A. D. Watt, N. E. Stork, and M. D. Hunter, pp. 109–134, Chapman and Hall, London.

Bird, M. I., J. G. Wynn, G. Saiz, C. M. Wurster, and A. McBeath (2015), The pyrogenic carbon cycle, *Annu. Rev. Earth Planet. Sci.*, *43*, 9.1–9.26.

Bleher, B., D. Uster, and T. Bergsdorf (2006), Assessment of threat status and management effectiveness in Kakamega Forest, Kenya, in *Forest Diversity and Management*, pp. 99–117, Springer, New York.

Bonachela, J. A., R. M. Pringle, E. Sheffer, T. C. Coverdale, J. A. Guyton, K. K. Caylor, S. A. Lavin, and C. E. Tarnita (2015), Termite mounds increase the robustness of dryland ecosystems to climate change, *Science*, *347*(6), 651–655.

Bond, W. J., F. I. Woodward, and G. F. Midgly (2005), The global distributions of ecosystems in a world without fire, *New Phytol.*, *165*, 525–538.

Brewer, C. E., K. Schmidt - Rohr, J. A. Satrio, and R. C. Brown (2009), Characterization of biochar from fast pyrolysis and gasification systems, *Environ. Prog. Sustain. Energ.*, *28*(3), 386–396.

Breznak, J. (2000), Ecology of prokaryotic microbes in the guts of wood-and litter-feeding termites, in *Termites: Evolution, Sociality, Symbioses, Ecology*, edited by T. Abe et al., pp. 209–231, Kluwer, Dordrecht.

Brodowski, S., B. John, H. Flessa, and W. Amelung (2006), Aggregate-occluded black carbon in soil, *Eur. J. Soil Sci.*, *57*(4), 539–546.

Brodowski, S., W. Amelung, L. Haumaier, and W. Zech (2007), Black carbon contribution to stable humus in German arable soils, *Geoderma*, *139*(1), 220–228.

Cheng, C. H., J. Lehmann, J. E. Thies, and S. D. Burton (2008), Stability of black carbon in soils across a climatic gradient, *J. Geophys. Res.*, *113*, JG000642, doi:10.1029/2007JG000642.

Crutzen, P. J., and M. O. Andreae (1990), Biomass burning in the tropics: Impact on atmospheric chemistry and biogeochemical cycles, *Science*, *250*(4988), 1669–1678.

Czimczik, C. I., and C. A. Masiello (2007), Controls on black carbon storage in soils, *Global Biogeochem. Cycles*, *21*, GB3005, doi:10.1029/2006GB002798.

Dai, X., T. Boutton, B. Glaser, R. Ansley, and W. Zech (2005), Black carbon in a temperate mixed-grass savanna, *Soil Biol. Biochem.*, *37*(10), 1879–1881.

Dittmar, T., C. E. de Rezende, M. Manecki, J. Niggemann, A. R. C. Ovalle, A. Stubbins, and M. C. Bernardes (2012), Continuous flux J., of dissolved black carbon from a vanished tropical forest biome, *Nat. Geosci.*, *5*(9), 618–622.

Food and Agricultural Organization (2014), *Background Information on Natural Resources in the Kagera River Basin*, The Food and Agricultural Organization of the United Nations, Rome, Italy.

Foereid, B., J. Lehmann, and J. Major (2011), Modeling black carbon degradation and movement in soil, *Plant Soil*, *345*, 223–236.

Forbes, M., R. Raison, and J. Skjemstad (2006), Formation, transformation and transport of black carbon (charcoal) in terrestrial and aquatic ecosystems, *Sci. Total Environ.*, *370*(1), 190–206.

Geist, H. J., and E. F. Lambin (2002), Proximate causes and underlying driving forces of tropical deforestation tropical forests are disappearing as the result of many pressures, both local and regional, acting in various combinations in different geographical locations, *BioScience*, *52*(2), 143–150.

Glenday, J. (2006), Carbon storage and emissions offset potential in an East African tropical rainforest, *Forest Ecol. Manage.*, *235*(1), 72–83.

Goldberg, E. D. (1985), *Black Carbon in the Environment: Properties and Distribution*, John Wiley, New York.

Guggenberger, G., A. Rodionov, O. Shibistova, M. Grabe, O. A. Kasansky, N. Fuchs, N. Mikheyeva, G. Zrazhevskaya, and H. Flessa (2008), Storage and mobility of black carbon in permafrost soils of the forest tundra ecotone in Northern Siberia, *Global Change Biol.*, *14*, 1367–1381.

Hertel, D., G. Moser, H. Culmsee, S. Erasmi, V. Horna, B. Schuldt, and C. Leuschner (2009), Below-and above-ground biomass and net primary production in a paleotropical natural forest (Sulawesi, Indonesia) as compared to neotropical forests, *Forest Ecol. Manage.*, *258*(9), 1904–1912.

Hockaday, W. C., A. M. Grannas, S. Kim, and P. G. Hatcher (2006), Direct molecular evidence for the degradation and mobility of black carbon in soils from ultrahigh-resolution mass spectral analysis of dissolved organic matter from a fire-impacted forest soil, *Org. Geochem.*, *37*(4), 501–510.

Huggett, R. J. (1998), Soil chronosequences, soil development, and soil evolution: A critical review, *Catena*, *32*, 155–172.

Jaffé, R., Y. Ding, J. Niggemann, A. V. Vähätalo, A. Stubbins, R. G. Spencer, J. Campbell, and T. Dittmar (2013), Global charcoal mobilization from soils via dissolution and riverine transport to the oceans, *Science*, *340*(6130), 345–347.

Jauss, V., M. Johnson, E. Krull, M. Daub, and J. Lehmann (2014), Pyrogenic carbon controls across a soil catena in the Pacific Northwest, *Catena*, *124*, 53–59.

Johnson, M. S., J. Lehmann, E. C. Selva, M. Abdo, S. Riha, and E. G. Couto (2006), Organic carbon fluxes within and streamwater exports from headwater catchments in the southern Amazon, *Hydrol. Process.*, *20*(12), 2599–2614.

Jones, J. A. (1990), Termites, soil fertility and carbon cycling in dry tropical Africa: A hypothesis, *J. Trop. Ecol.*, *6*(03), 291–305.

Joseph, S., M. Camps-Arbestain, Y. Lin, P. Munroe, C. Chia, J. Hook, L. Van Zwieten, S. Kimber, A. Cowie, and B. Singh (2010), An investigation into the reactions of biochar in soil, *Soil Res.*, *48*(7), 501–515.

Kimetu, J. M., J. Lehmann, S. O. Ngoze, D. N. Mugendi, J. M. Kinyangi, S. Riha, L. Verchot, J. W. Recha, and A. N. Pell (2008), Reversibility of soil productivity decline with organic matter of differing quality along a degradation gradient, *Ecosystems*, *11*(5), 726–739.

Knicker, H., R. Nikolova, D. P. Dick, and R. S. D. Dalmolin (2012), Alteration of quality and stability of organic matter in grassland soils of Southern Brazil highlands after ceasing biannual burning, *Geoderma*, *181*, 11–21.

Kuhlbusch, T. A. J., and P. J. Crutzen (1995), Toward a global estimate of black carbon in residues of vegetation fires representing a sink of atmospheric CO_2 and a source of O_2, *Global Biogeochem. Cycles*, *9*(4), 491–501, doi:10.1029/95GB02742.

Kuhlbusch, T. A. J., M. O. Andreae, H. Cachier, H. Goldammer, J. P. Lacaux, R. Shea, and P. J. Crutzen (1996), Black carbon formation by savanna: Measurements and implications for the global carbon cycle, *J. Geophys. Res.*, *101*(D19), 23,651–23,665, doi:10.1029/95JD02199.

Lehmann, J., J. O. Skjemstad, S. Sohi, J. Carter, M. Barson, P. Falloon, K. Coleman, P. Woodbury, and E. Krull (2008), Australian climate–carbon cycle feedback reduced by soil black carbon, *Nat. Geosci.*, *1*(12), 832–835.

Lehmann, J., S. Abiven, M. Kleber, G. Pan, B. P. Singh, S. Sohi, and A. Zimmerman (2015), Persistence of biochar in soil, in *Biochar for Environmental Management: Science, Technology and Implementation*, edited by J. Lehmann and S. Joseph, pp. 235–282, Taylor and Francis, London.

Leifeld, J., S. Fenner, and M. Müller (2007), Mobility of black carbon in drained peatland soils, *Biogeosciences*, *4*(3), 425–432.

Liang, B., J. Lehmann, D. Solomon, S. Sohi, J. E. Thies, J. O. Skjemstad, F. J. Luizao, M. H. Engelhard, E. G. Neves, and S. Wirick (2008), Stability of biomass-derived black carbon in soils, *Geochim. Cosmochim. Acta*, *72*(24), 6069–6078.

Major, J., J. Lehmann, M. Rondon, and C. Goodale (2010), Fate of soil-applied black carbon: Downward migration, leaching and soil respiration, *Global Change Biol.*, *16*(4), 1366–1379, doi:10.1111/j.1365-2486.2009.02044.x.

Mbagwu, J. (1997), Quasi-steady infiltration rates of highly permeable tropical moist savannah soils in relation to landuse and pore size distribution, *Soil Technol.*, *11*(2), 185–195.

Meredith, W., P. L. Ascough, M. I. Bird, D. J. Large, C. E. Snape, Y. Sun, and E. L. Tilston (2012), Assessment of hydropyrolysis as a method for the quantification of black carbon using standard reference materials, *Geochim. Cosmochim. Acta*, *97*, 131–147.

Müller, D., and J. Mburu (2009), Forecasting hotspots of forest clearing in Kakamega Forest, western Kenya, *Forest Ecol. Manage.*, *257*(3), 968–977.

Mutie, S. M., B. Mati, O. Home, H. Gadain, and J. Gathenya (2006), Evaluating land use change effects on river flow using USGS geospatial stream flow model in Mara River basin, Kenya, in *Center for Remote Sensing of Land Surfaces*, pp. 141–148, Bonn, Germany.

Nguyen, B. T., J. Lehmann, J. Kinyangi, R. Smernik, S. J. Riha, and M. H. Engelhard (2008), Long-term black carbon dynamics in cultivated soil, *Biogeochemistry*, *89*(1–2), 295–308.

Okello, B. D., T. G. O'Connor, and T. P. Young (2001), Growth, biomass estimates, and charcoal production of Acacia drepanolobium in Laikipia, Kenya, *Forest Ecol. Manage.*, *142*, 143–153.

Okungu, J., and P. Opango (2012), *Pollution Loads Into Lake Victoria From the Kenyan Catchment*, edited by E. A. Commission, Lake Victoria Environmental Management Project (LVEMP), Kisumu, Kenya.

Polyakov, V., and R. Lal (2004), Modeling soil organic matter dynamics as affected by soil water erosion, *Environ. Int.*, *30*(4), 547–556.

Ramanathan, V., and G. Carmichael (2008), Global and regional climate changes due to black carbon, *Nat. Geosci.*, *1*(4), 221–227.

Recha, J. W. (2011), Streamwater dynamics and carbon and nutrient losses in tropical headwater catchments at a soil degradation gradient. PhD thesis, Cornell Univ.

Recha, J. W., J. Lehmann, M. T. Walter, A. Pell, L. Verchot, and M. Johnson (2012), Stream discharge in tropical headwater catchments as a result of forest clearing and soil degradation, *Earth Interact.*, *16*(13), 1–18, doi:10.1175/2012EI000439.1.

Recha, J. W., J. Lehmann, M. T. Walter, A. Pell, L. Verchot, and M. Johnson (2013), Stream water nutrient and organic carbon exports from tropical headwater catchments at a soil degradation gradient, *Nutr. Cycling Agroecosyst.*, *95*, 145–158.

Renck, A., and J. Lehmann (2004), Rapid water flow and transport of inorganic and organic nitrogen in a highly aggregated tropical soil, *Soil Sci.*, *169*(5), 330–341.

Riedel, T., S. Iden, J. Geilich, K. Wiedner, W. Durner, and H. Biester (2014), Changes in the molecular composition of organic matter leached from an agricultural topsoil following addition of biomass-derived black carbon (biochar), *Org. Geochem.*, *69*, 52–60.

Rumpel, C., V. Chaplot, O. Planchon, J. Bernadou, C. Valentin, and A. Mariotti (2006a), Preferential erosion of black carbon on steep slopes with slash and burn agriculture, *Catena*, *65*(1), 30–40.

Rumpel, C., M. Alexis, A. Chabbi, V. Chaplot, D. Rasse, C. Valentin, and A. Mariotti (2006b), Black carbon contribution to soil organic matter composition in tropical sloping land under slash and burn agriculture, *Geoderma*, *130*(1), 35–46.

Rwetabula, J., F. De Smedt, and M. Rebhun (2007), Prediction of runoff and discharge in the Simiyu River (tributary of Lake Victoria, Tanzania) using the WetSpa model, *Hydrol. Earth Syst. Sci. Discuss.*, *4*(2), 881–908.

Sangale, F., J. Okungu, and P. Opango (2012), *Variation of Flow of Water From Rivers Nzoia, Yala and Sio Into Lake Victoria*, Lake Victoria Basin Commission, Kisumu, Kenya.

Schluter, T., and C. Hampton (1997), *Geology of East Africa*, Borntraeger, Berlin, Germany.

Schmidt, M. W., and A. G. Noack (2000), Black carbon in soils and sediments: Analysis, distribution, implications, and current challenges, *Global Biogeochem. Cycles*, *14*, 777–793, doi:10.1029/1999GB001208.

Schmidt, M. W. I. (2004), Biogeochemistry: Carbon budget in the black, *Nature*, *427*, 305–307.

Schmidt, M. W. I., J. O. Skjemstad, E. Gehrt, and I. Kögel-Knabner (1999), Charred organic carbon in German chernozemic soils, *Eur. J. Soil Sci.*, *50*, 351–365.

Skjemstad, J. O., D. C. Reicosky, A. R. Wilts, and J. A. McGowen (2002), Charcoal carbon in U.S. agricultural soils, *Soil Sci*, *Soc. Am. J.*, *66*, 1249–1255.

Solomon, D., et al. (2007), Long-term impacts of anthropogenic perturbations on the dynamics and molecular speciation of organic carbon in tropical forest and subtropical grassland ecosystems, *Global Change Biol.*, *13*, 511–530.

Sombroek, W. G., H. Braun, and B. J. A. Pouw (1982), Exploratory soil map and agro-climatic zone map of Kenya, 1980, Exploratory Report-Kenya Soil Survey Ministry of Agriculture, Nairobi, Kenya.

Terhoeven-Urselmans, T., T. Gunnar-Vagen, O. Spaargaren, and K. D. Shepherd (2010), Prediction of soil fertility properties from a globally distributed soil mid-infrared spectral library, *Soil Sci. Soc. Am. J.*, *74*, 1792–1799.

Tsingalia, H. M., and F. N. Kassily (2009), The origins Kakamega Forest grasslands: A critical review, *J. Hum. Ecol.*, *27*, 129–135.

Walling, D., and B. Webb (1980), The spatial dimension in the interpretation of stream solute behavior, *J. Hydrol.*, *47*(1), 129–149.

Wass, P. (1995), *Kenya's Indigenous Forests: Status, Management, and Conservation*, World Conservation Union, Gland, Switzerland.

Wurster, C. M., G. Saiz, M. Schneider, M. Schmidt, and M. I. Bird (2013), Quantifying pyrogenic carbon from thermosequences of wood and grass using hydrogen pyrolysis, *Org. Geochem.*, *62*, 28–32.